A QUANTITATIVE STUDY OF TAU PATHOLOGY IN ELEVEN CASES OF CHRONIC TRAUMATIC ENCEPHALOPATHY

Richard A. Armstrong,[1] Ann C. McKee,[2,3],[4],Thor D. Stein, [4,5,] Victor E. Alvarez[3,5,] and Nigel J. Cairns[6]

[1]Vision Sciences, Aston University, Birmingham B4 7ET, UK;

[2]VA Boston HealthCare System, Boston MA, 02130, USA

[3]Department of Neurology, Boston University School of Medicine, Boston, MA, 02118, USA;

[4]Department of Pathology & Laboratory Medicine, Boston University School of Medicine, Boston, MA, 02118, USA;

[5]Department of Veterans Affairs Medical Center, Bedford, MA, 01730, USA;

[6]Departments of Neurology and Pathology & Immunology, Washington University School of Medicine, Saint Louis, Missouri 63110, USA.

Corresponding author: Dr. RA Armstrong, Vision Sciences, Aston University, Birmingham B4 7ET, UK (Tel: 0121-204-4102; Fax: 0121-204-3892; Email: R.A.Armstrong@aston.ac.uk)

Running Head: Quantitative pathology of chronic traumatic encephalopathy

Key Words: Chronic traumatic encephalopathy (CTE); Tau; Neurofibrillary tangles (NFT); Astrocytic tangles (AT); Principal components analysis (PCA)

Number of words: 8026

Number of Tables: 4

Number of Figures: 9

Abstract

Aims: To quantify tau pathology of chronic traumatic encephalopathy (CTE) and investigate influence of dot-like lesions (DL), brain region, co-morbidity, and sporting career length. **Methods**: Densities of neurofibrillary tangles (NFT), astrocytic tangles (AT), DL, oligodendroglial inclusions (GI), neuropil threads (NT), vacuoles, neurons, and enlarged neurons (EN) were measured in tau-immunoreactive sections of upper cortical laminae of frontal and temporal lobe, hippocampus (HC), amygdala, and substantia nigra (SN) of eleven cases of CTE. **Results**: DL were a consistent finding in CTE. Densities of NFT, NT and DL were greatest in sectors CA1 and CA2 of the HC. Densities of AT were lower than NFT, small numbers of GI were recorded in temporal lobe, and low densities of vacuoles and EN were consistently present. β-amyloid containing neuritic plaques (NP) also occurred at low density. Densities of NFT, NT, DL, and AT were greater in sulci than gyri while vacuole density was greater in gyri. Principal components analysis (PCA) suggested that sporting career length and densities of NFT in entorhinal cortex, NT in CA2 and SN, and vacuolation in the DG were significant sources of variation among cases. **Conclusion**: DL are frequent in CTE suggesting affinity with argyrophilic grain disease (AGD) and Parkinson's disease dementia (PD-Dem). Densities of AT in all regions and NT/DL in sectors CA2/4 were consistent features of CTE. The eleven cases are neuropathologically heterogeneous which may result from genetic diversity, and variation in anatomical pathways subjected to trauma.

List of abbreviations:

AD	Alzheimer's disease
ADNC	Alzheimer's disease neuropathologic change
AGD	Argyrophilic grain disease
ANOVA	Analysis of variance
AT	Astrocytic tangle
CBD	Corticobasal degeneration
CTE	Chronic traumatic encephalopathy
DG	Dentate gyrus
DL	Dot-like lesions
EC	Entorhinal cortex
EN	Enlarged neuron
HC	Hippocampus
HS	Hippocampal sclerosis
GI	Oligodendroglial inclusion
NFL	National football league
NFT	Neurofibrillary tangle
NIA-AA	National Institute on Aging-Alzheimer's Association
NP	Neuritic plaque
NT	Neuropil thread
PART	Primary age-related tauopathy
PCA	Principal components analysis
PD-Dem	Parkinson's disease dementia
PiD	Pick's disease
PSP	Progressive supranuclear palsy
SFG	Superior frontal gyrus
SN	Substantia nigra
STG	Superior temporal gyrus
TDP-43	Transactive response DNA-binding protein of 43kDa

Introduction

Mortality from neurodegenerative disease, including Alzheimer's disease (AD) and amyotrophic lateral sclerosis (ALS), among retired National Football League (NFL) players is over three times that recorded in the general population [1]. In addition, chronic traumatic encephalopathy (CTE) is a neurodegenerative disorder believed to result from repetitive brain injury [2,3]. CTE has been recorded in association with a variety of physical activities including such contact sports as boxing, American football, ice hockey, and wrestling [4] and has also been reported in military veterans exposed to blast shock waves from explosive devices [5-8]. Although controversial [9,10], a history of mild traumatic brain injury appears to be the only risk factor consistently associated with CTE [4].

Clinically, the symptoms of CTE include impairment of memory and executive function, behavioural change, disturbances of mood, and the presence of motor symptoms [11,12] initially recognized two relatively distinct clinical subtypes of CTE presenting with either changes in behavior or mood, most frequently found in younger individuals, or with changes in cognition, which is more characteristic of older patients. Subsequently, four clinical subtypes of the disease were proposed characterized by: (1) changes in behaviour and mood, (2) declining cognition, (3) a 'mixed' syndrome, and (4) a profound dementia [13]. In addition, in one of the largest studies to date of retired NFL players, Mckee et al [14] identified four stages in the clinical development of CTE characterized by: (1) headache, loss of attention, and consciousness, (2) depression, explosivity, and short-term memory loss, (3) loss of executive function and cognition, and (4) dementia. The stage of tau pathology present was related to duration of playing career, survival after retirement, and age at death [6].

The gross neuropathology of CTE frequently overlaps with that of common neurodegenerative disease such as AD [4]. CTE cases exhibit reduced gray matter volume in several brain regions, most prominently affecting frontal and anterior temporal lobes and often associated with enlargement of the lateral and third ventricles [6,14]. A spectrum of tau-imunoreactive pathology is present which varies from focal, perivascular neurofibrillary tangles (NFT) in frontal cortex [15] to a more

widespread and severe tauopathy affecting temporal lobe, limbic system, and the striato-nigral system [6]. The isoform profile and phosphorylation state of tau in CTE is similar to that of AD in that both three-repeat (3R) and four-repeat (4R) tau are present in equal ratios [16]. NFT and neuropil threads (NT) can be observed in affected areas together with comorbid AD neuropathologic change (ADNC), viz. β-amyloid neuritic plaques (NP) [17,18], and astrocytic tangles (AT) [11,19]. In addition, the presence of dot-like lesions (DL) was reported in CTE by McKee et al [14] resembling the argyrophilic grains (AG) commonly observed in several conditions including argyrophilic grain disease (AGD) [21-24], Alzheimer's disease (AD) [25], and cognitively normal aged brains [26,27] but have not been investigated to date in CTE. Oligodendroglial inclusions (GI), abnormally enlarged neurons (EN), and vacuolation have also been recorded in several tauopathies and may also be present in CTE. In addition to tau and β-amyloid pathology, transactive response (TAR) DNA-binding protein of 43kDa (TDP-43)-immunoreactive pathology [11,15,19] has been observed in a significant number of CTE cases as neuronal cytoplasmic inclusions (NCI) and dot-like structures with a distribution similar to that of frontotemporal dementia with TDP-43-immunoreactive inclusions [28,29].

The present study quantified tau-immunoreactive NFT, NT, DL, NP, AT, and GI together with vacuoles, neurons, and EN in regions of frontal and temporal lobe and in the SN of 11 cases of CTE with the following specific objectives: (1) to compare densities of pathological changes among regions, (2) to determine the relative abundance of neuronal and glial pathologies, (3) to determine the pathological importance of GR, EN, and vacuoles, (4) to compare densities of the pathology in crests/sides of gyri within the depths of the sulci, and (5) using principal components analysis (PCA) [29], to determine the degree of heterogeneity among cases and the most important sources of neuropathological variation. In addition, as ADNC co-pathology is commonly reported in CTE [11,19], the CTE data were compared with ADNC cases not associated with CTE, but with a similar degree of AD pathology [30].

Materials and Methods

Cases

CTE cases (n = 11, mean age 70 years, SD = 6.42) and ADNC cases not associated with CTE (n = 7, mean age 79 years, SD = 8.83) (Table 1) were obtained from the Boston University Alzheimer's Disease Center CTE Program Brain Bank, Boston University School of Medicine, Boston, MA, USA. ADNC cases without CTE had a higher average age and SD compared with the CTE cases but a similar pathology, National Institute on Aging-Alzheimer's (NIA-AA) association guidelines 'ABC' scores equating to 'not AD' - 'intermediate' probability of AD [30]. With the exception of one CTE case, a boxer for 26 years (Case C), all individuals had played American football, with career durations varying from 11-24 years. In addition, all subjects had suffered at least one concussion, associated with variable loss of consciousness; the majority of subjects having experienced multiple episodes of trauma during their athletic careers. One case was diagnosed as 'pure' CTE without any associated co-morbidity but the remaining cases exhibited one or more co-pathologies most commonly ADNC (N = 7), primary age-related tauopathy (PART) (N = 2), hippocampal sclerosis (HS) (N = 4), TDP-43 immunoreactive pathology (N = 8), or AGD (N = 1). Inclusion criteria for cases were according to McKee et al. [14,31]. The most important diagnostic criterion is the presence of abnormally phosphorylated tau (p-tau) aggregates in neurons, astrocytes, and cell processes and located around small vessels in an irregular pattern in the depths of cortical gyri. In addition, supportive criteria include: (1) abnormal p-tau- immunoreactive pre-NFT and NFT in superficial cortical laminae II/III, sector CA2 of the hippocampus, and proximal dendritic swellings in sector CA4, (3) abnormal p-tau aggregates in mammillary bodies, hypothalamic nuclei, amygdala, nucleus accumbens, midbrain tegmentum, nucleus basalis, substantia nigra, and locus caeruleus, (4) p-tau-immunoreactive astrocytes at glial limitans, and (5) p-tau-immunoreactive grain-like or DL lesions. PART is a new neuropathological entity which describes tau pathology in the temporal lobe associated with aging independent of amyloid pathology [32,33]. Hence, cases diagnosed as CTE were also designated as having PART according to the following inclusion criteria: (1) a diffuse cerebral atrophy was present most severe in the temporal lobe, (2) NFT were present in the medial temporal lobe, hippocampus, and amygdala, (3) extracellular 'ghost' tangles were present, and (4) sparse diffuse β-amyloid deposits were present but with very few NP [32].

Neuropathology

All procedures performed in these studies were in accordance with the ethical standards of the institutional Review Board of Boston University and were carried out according to the 1964 Declaration of Helsinki and later amendments. After death, the next-of-kin provided written consent for brain removal and retention for research studies. Brains were fixed in ice cold periodate-lysine paraformaldehyde for at least two weeks, paraffin-embedded, and sections cut at 6 μm. For this study, blocks were taken from: (1) frontal lobe to study the superior frontal gyrus (SFG) (BA 8,6), (2) temporal pole (BA 38,36) (3) superior temporal gyrus (STG) (BA 22), (4) medial temporal lobe to study entorhinal cortex (EC) (BA 28) and the amygdala, (5) HC to study the subiculum, sectors CA1-4, and the dentate gyrus (DG), and (6) midbrain to study the SN. Histologic stains included Luxol fast blue counterstained with hematoxylin and eosin (LHE) and a modified Bielschowsky silver impregnation. Immunohistochemistry was performed using the following antibodies: Aβ42 (AB5078P; EMD Millipore, Billerica, MA, USA; 1:2000), phosphorylated tau (AT8, Pierce Endogen, Rockford, IL, USA; 1:2000), and phosphorylated TDP-43 (pTDP-43, pS409/410 mouse monoclonal; Cosmo Bio Co, Tokyo, Japan; 1:2000). Each slide was scanned and subsequently visualized on a personal computer (PC) using Aperio Image-Scope Software (Leica Biosystems Inc. Buffalo Grove, IL, USA).

Morphometric methods

In each cortical region (SFG, TP, STG, EC), the densities of NFT, NT, DL, NP, AT, GI, vacuoles, neurons, and EN (Figs 1-4), were measured along a strip of tissue parallel to the pia mater, using 250 x 50 μm sample fields arranged contiguously and superimposed over the tau-immunoreactive image using either the draw or rectangle options. The sample fields were located in the upper (approximating to laminae II/III) cortex, the region where tau-pathology of CTE is most evident [6,34]. The short edge of the sample field was orientated parallel with the pia mater and aligned with guidelines also marked on the section. Sample fields were located first, commencing on the crest and extending to the upper side of the gyrus (N = 32 fields) and second, in the depths of the adjacent sulcus (N = 16 fields). In the HC, the histological features were counted in the subiculum (N = 16 fields) and in sectors CA1, CA2, CA3, and

CA4, (N = 16 fields for CA1, and N = 8 fields for other sectors) the short dimension of the sample field being aligned with the alveus to sample CA1, CA2, and CA3. Measurements were then continued into sector CA4 using a guideline marked on the section and which ceased approximately 400 μm from the DG fascia. In the DG, the pathology was quantified in the molecular and granule cell layer (N = 32 fields). In the amygdala (N = 16 fields), the fields were arranged across the maximum diameter of the basolateral nucleus, a region in which a particular concentration of tau pathology was observed. In the midbrain, fields were aligned along the lower edge of the crus cerebri to sample the SN as far as the corticonigral fibres (N = 16 fields).

All NFT, NT, DL, AT, GI, NP, EN, surviving neurons and vacuoles were counted within each sample field. NT were thread-like structures some of which were serpiginous, while small circular structures were identified as DL (Fig 1). AT (Fig 2) and GI (Fig 3) were clearly associated with glial cell nuclei, the former with larger, pale nuclei and the latter with small, dark nuclei, while NFT were present in the cytoplasm of larger cells with a distinct region of haematoxylin-positive cytoplasm. Neurons with an abnormally enlarged perikaryon and a nucleus displaced to the periphery of the cell were regarded as EN (Fig 3). Surviving neurons were identified as cells containing at least some stained cytoplasm in combination with larger shape and non-spherical outline. The number of discrete vacuoles (Fig 4) present in the neuropil greater than 5 μm in diameter was also recorded in each sample field. It can be difficult to differentiate microvacuolation of the neuropil from vacuolation around neurons and blood vessels attributable to artifacts of processing. Hence, vacuoles clearly associated with such structures were not counted.

Data analysis

The data were analyzed by analysis of variance (ANOVA) (STATISTICA software, Statsoft Inc., Tulsa, OK, USA). First, mean densities of each histological feature in crests/sides of gyri of cortical regions were compared with those in the subiculum, CA sectors of the HC, amygdala, DG, and SN using two-way (cases x regions) ANOVA. Subsequent comparisons among brain regions were made using Tukey's *post-hoc* test. Second, in cortical regions numerical densities of each histological feature were compared between gyri and sulci using two-factor, split-plot ANOVA

[35,]. Third, CTE/ADNC cases were compared with ADNC cases not associated with CTE using a two-factor repeated measures ANOVA. Fourth, to study pathological heterogeneity among the 11 CTE cases, the data were analysed using principal components analysis (PCA) [29]. Two separate analyses were carried out using the CTE cases as variables and the histological measurements as defining features: (1) PCA-1 based on the spectrum of histological features: NFT, NT, DL, AT, GI, NP, EN, surviving neurons, vacuoles, and (2) PCA-2 based on the tau-immunoreactive pathology alone. The result of a PCA is a scatter plot of the cases in relation to the extracted principal components (PC) in which the distance between cases reflects their relative similarity or dissimilarity based on the defining histological features. Such a plot can reveal whether neuropathological variation is continuously distributed or whether discrete clusters of cases are present. To correlate the location of a case on a PC axis with the numerical density of a specific neuropathological feature, correlations (Pearson's 'r') were calculated between the densities of each histological feature of each CTE case and the factor loadings of the case relative to the PC1 and PC2. For example, a significant correlation between the density of a feature and PC1 would identify that feature as important in determining the separation of cases along PC1.

Results

The numerical densities of the NFT, NT, DL and NP in each brain region, averaged over cases, are shown in Fig 5. Densities of the DL were 2-3 times and up to 20 times those of NT and NFT respectively. In a random sample of cortical DL (N = 565), mean diameter was 1.80 μm (Median = 2 μm, Mode = 2 μm, range 1 - 6 μm, SD = 0.84 μm). The ANOVA suggested significant differences in density of NFT ($F = 4.42$, $P < 0.001$), NT ($F = 3.49$, $P < 0.001$), and DL ($F = 4.56$, $P < 0.001$) among regions with greatest densities in sectors CA1/2 compared with most other regions. Low densities of NP were present in seven cases and were present largely in the temporal lobe. Densities of the AT ($F = 1.58$, $P > 0.05$) and GI ($F = 1.10$, $P > 0.05$) (Fig 6) were significantly lower than NFT and there were no statistically significant differences among regions. In addition, low densities of EN were present in all regions with the exception of the DG (Fig 7), greatest densities being observed in sector CA2, the amygdala, and SN ($F = 6.81$, $P < 0.001$). A significant difference in vacuolation was

also present among regions ($F = 3.81$, $P < 0.001$) with greatest densities in the temporal pole and STG.

In cortical regions, there were significant differences in density of tau-immunoreactive pathology between the crests/sides of the gyri and depths of the sulci (Table 2). Hence, for NFT (region x location: $F = 6.64$, $P < 0.001$) and NT (region x location: $F= 7.11$, $P < 0.001$), densities in sulci were greater than in gyri but only in the SFG whereas densities of DL were significantly greater in sulci versus gyri in all cortical regions studied ($F = 4.06$, $P < 0.05$). There were greater densities of AT ($F = 4.61$, $P < 0.05$) in gyri than sulci but no significant differences in GI with location ($F = 1.02$, $P > 0.05$). In addition, there were no significant differences in density of EN between gyri and sulci ($F = 0.10$, $P > 0.05$), but the density of vacuoles was greater in gyri than sulci in all cortical regions ($F = 10.59$, $P < 0.01$).

A comparison of the densities of histological variables in CTE and ADNC cases is shown in Table 3. The ANOVA suggest that only the AT ($F = 5.26$, $P < 0.05$), and NP ($F = 13.28$, $P < 0.01$) were significantly different between case groups across all regions, the density of AT being greater in CTE and NP in AD. In addition, significant case groups x brain region interactions suggested: (1) density of NT were greater in ADNC in the STG and amygdala and greater in CTE in sectors CA2 and CA4 ($F = 2.02$, $P < 0.01$) and (2) densities of DL were greater in CTE in the SFG and in sectors CA2 and CA4, ($F = 2.49$, $P < 0.01$).

A PCA of the density data based on all histological variables (PCA-1) resulted in the extraction of two PC's accounting in total for 80% of the variance (PC1 = 73%, PC2 = 8%). A plot of the eleven cases in relation to PC1 and PC2 is shown in Fig 8 and the significant correlations between the factor loadings of the cases on the PC and neuropathological variables in Table 4. The cases with relatively little co-pathology, i.e., 'pure' CTE and CTE/PART are located towards the bottom right of the plot while cases distributed to the left and upper part of the plot exhibit a greater degree of co-pathology. Neither cases with ADNC or TDP-43 co-pathology segregate in relation to PC1/2. The data suggest: (1) PC1 negatively correlates with the density of NT in sectors CA2/4 and the SN, and vacuolation in the DG and (2) PC1 positively correlates with the densities of NFT and DL in CA1 and surviving neurons in DG. In

addition, career length was negatively correlated with PC2 ($r = -0.75$, $P < 0.01$) but there were no correlations between frequency of concussions and either PC. A PCA of the density data based on the tau-immunoreactive pathology alone (PCA-2) also resulted in the extraction of two PC's accounting for a total of 83% of the total variance (PC1 = 75%, PC2 = 8%). A plot of the eleven cases in relation to PC1 and PC2 is shown in Fig 9 and the correlations between the factor loadings of the cases on the PC and neuropathological variables in Table 2. The data suggest: (1) PC1 positively correlates with the density of NFT in EC gyri and negatively correlates with the density of NT in sector CA2 and (2) PC1 positively correlates with the densities of NFT in sector CA1 and negatively correlates with DL in sector CA1. In addition, sporting career length was negatively correlated with PC1 ($r = -0.67$, $P < 0.05$) and PC2 ($r = -0.75$, $P < 0.01$).

Discussion

The data suggest that the eleven cases of CTE studied are characterized by the presence of NFT, NT, and abundant DL in multiple regions with mean densities of the NT and DL being significantly greater than those of NFT in all regions. Among brain regions: (1) NFT, NT, and DL affected most regions studied but were most abundant in sectors CA1 and CA2 of the HC, the SFG and DG being least affected, (2) AT and small numbers of GI were present but at significantly lower densities than NFT, (3) EN and vacuolation were present, the former at low densities in sector CA2, amygdala and SN and the latter in cortical regions, especially the TP and STG, and (4) pathological changes, especially DL and NT, were generally greater in sulci than gyri, whereas NFT and AT were more abundant in sulci in SFG only. EN are present at low density in the majority of disorders and therefore, not a specific feature of CTE. Hence, DL are a widespread additional feature of the pathology of CTE and these data suggest similarities between CTE and other disorders in which grain pathology is abundant, such as AGD, another tauopathy, and Parkinson's disease dementia (PD-Dem), a synucleinopathy [36]. Nevertheless, the range of DL size is less than the 4 - 8 μm usually quoted for grains in AGD [22] raising the question as to the whether these lesions are analogous to those of AGD. In addition, DI have a different distribution in CTe, PDD, and AGD being present at highest density in CTE ibn sectors CA1/2 of

ther hippocampus, CA2 in PDD [36] and the subiculum and CA 1 in AGD (R.A. Armstrong, unpublished data.

The densities of NFT were greater in CTE than NCI in other tauopathies with comparable quantitative data such as Pick bodies (PB) in Pick's disease (PiD) [37], and NCI in corticobasal degeneration (CBD) [38], but less than the NFT in AD [39]. Within the HC, densities of NFT were greatest in sectors CA1/2, lower densities being present in the EC, subiculum, CA1, CA4, and the DG, a similar distribution to that present in CBD [39]. The distribution of pathology in the HC differs between CTE and PiD, where characteristically large numbers of PB were present in DG granule cells in PiD [39]. In addition, in both AD and PSP, greater densities of NFT were observed in CA1 compared with CA2 [39], whereas densities were comparable in these regions in CTE. The distribution of the NT and DL in CTE is generally similar to that of the NFT with 2-3 and up to 20 times more NT and DL respectively than NFT. The only comparable quantitative data for such pathologies are for the synucleinopathy PD-Dem in which neurites and grains were present at 10 and 25 times the density of Lewy bodies (LB) respectively [36]. The densities of glial inclusions were low in laminae II/III of the cortex. However, AT have been reported fairly widely in CTE [11] with focal aggregations around larger blood vessels and in lamina I, especially in the depths of the sulci [15].

A number of features of the pathology were present at higher density in the depths of the sulci compared with the crests and upper sides of the gyri as previously reported in CTE [14,15]. These differences in density were evident in all gyri studied but were most marked in frontal cortex where in some cases a marked perivascular distribution of NFT, NT, and DL was present [6,15]. This distribution is also shown by all morphological subtypes of Aβ deposit in AD and could reflect greater deposition of Aβ in sulci attributable to the higher density of neurons and penetrating blood vessels in this region [40,41]. However, there was little significant variation in neuronal densities between gyri and sulci in these cases, which may reflect greater neuronal loss in sulci. By contrast, vacuolation was less evident in the depths of the sulci compared with the gyri, which could reflect the more tightly packed cellular structure present in sulci.

ADNC is the most frequent co-pathology found in CTE [17,18]. Hence, comparing the densities of pathology in CTE in ADNC cases with and without CTE but with similar overall degrees of AD pathology may enable those pathological changes more characteristic of CTE to be identified. Hence, although densities are low in many areas, the presence of AT in multiple regions appears more characteristic of CTE, these lesions being rare in ADNC. In addition, densities of NT and DL are significantly higher in frontal cortex and sectors CA2 and CA4 in CTE than ADNC. Conversely, the density of NP is greater in ADNC especially in the cortex. Other common pathological changes, such as NFT and NT have similar densities in CTE and ADNC suggesting they may be largely attributable to ADNC while others, such as EN and GI, are relatively rare and non-specific, being observed in a variety of disorders

The results of the PCA suggest neuropathological heterogeneity among the CTE cases studied. The distribution of cases along PC1 positively correlates with densities of NFT in the EC (PCA-1) and negatively correlates with the densities of NT in sector CA2 (PCA-1 and PCA2) and sector CA4 (PCA-1), NT in the SN, and vacuolation in the DG. Hence, PC1 separates those cases with high densities of tau-immunoreactive pathology in the EC from those with higher densities of tau pathology in the HC. Similarly, PC2, although accounting for significantly less of the total variance, separates those cases with high densities of NFT in sector CA1 and less neuronal loss in the DG in the upper part of the plot from those with higher densities of DL in sector CA1 and greater neuronal loss in the DG. These pathological changes, especially along PC1 are also associated with an increase in the presence of various co-pathologies, most frequently AD, but also TDP-43, and HS. An interesting finding is the correlation between both PC1 and PC2 and career length when tau pathology only was included as defining variables [6]. Length of career may be a better predictor of resulting neuropathology as it includes sub-concussive levels of trauma and not just the frequency of reported concussions. In addition, recent research suggests that pathogenic proteins such as tau and α-synuclein can be secreted from cells, enter other cells, and seed small intracellular aggregates within these cells [42,43]. The frontal lobes may be especially vulnerable to trauma and hence, could be the initial site of tau pathology in CTE, with subsequent spreading to other regions via cell to cell transport resulting in a more widespread tauopathy [42]. Separation of cases

along the PC could therefore be explained by variations in the anatomical pathways of spread of tau-immunoreactive pathology in CTE.

In conclusion, the data suggest abundant and widespread tau pathology in the frontal and temporal lobes, and especially sectors CA1/2 in CTE. In particular, DL appear as a significant additional feature of the pathology. Compared with cases of ADNC which were not associated with CTE, the presence of AT in multiple regions and NT/DL pathology in sectors CA2 and CA4 appear to be a features of CTE rather than ADNC. By contrast, lower densities of AT and GI are present in temporal lobe and low densities of vacuoles and EN are present in most brain regions. There is also greater density of tau pathology in cortical sulci as previously reported. The eleven cases are neuropathologically heterogeneous which may result from many factors, including genetic diversity, other exposures, and variation in anatomical pathways subjected to trauma and subsequently, in cell to cell transfer of tau.

Acknowledgements

The authors gratefully acknowledge the use of the resources and facilities at the Edith Nourse Rogers Memorial Veterans Hospital (Bedford, MA, USA). We also gratefully acknowledge the help of all members of the Chronic Traumatic Encephalopathy Program at Boston University School of Medicine, VA Boston and the Bedford VA, as well as the individuals and families whose participation and contributions made this work possible. This work was supported by the National Institute of Neurological Disorders and Stroke (1UO1NS086659-01), Department of Veterans Affairs, the Veterans Affairs Biorepository (CSP 501), the Translational Research Center for Traumatic Brain Injury and Stress Disorders (TRACTS), Veterans Affairs Rehabilitation Research and Development Traumatic Brain Injury Center of Excellence (B6796-C), the National Institute of Aging Boston University Alzheimer's Disease Center (P30AG13846; supplement 0572063345–5). This work was supported by the Charles F. and Joanne Knight Alzheimer's Disease Research Center, Washington University School of Medicine, St. Louis, MO, USA (P50 AG05681 and P01 AG03991 from the National Institute on Aging. Contribution of listed authors: Richard Armstrong designed the project, carried out the quantitative studies, statistically analysed the data, and wrote the first draft of the article. Ann

McKee and Nigel Cairns collaborated in the design and in the preparation of the manuscript. Ann McKee, Thor Stein, and Victor Alvarez supplied images of the CTE cases using Aperio Image-Scope Software.

References

1 Lehman EJ, Hein MJ, Baron SL, Gersic CM. Neurodegenerative causes of death among retired National Football League players. Neurology 2012; 79: 1970-1974.doi:10.1212/WNL.0b013e3182daf50

2 Jordan BD. The clinical spectrum of sport-related traumatic brain injury. Nat Rev Neurol 2013; 9: 222-230.doi:10.1038/nrneural.2013.33

3 Geddes J, Vowles G, Nicoll J, Revesz T. Neuronal cytoskeletal changes are an early consequence of repetitive brain injury. Acta Neuropathol 1999; 98: 171-178.

4 Maroon JC, Winkelman R, Bost J, Amos A, Mathyssek C, Miele V. Chronic traumatic encephalopathy in contact sports: A systematic review of all reported pathological cases. PLOS ONE 2015; 10: e0117338.doi:10.1371/journal.pone.0130507

5 Goldstein LE, Fisher AM, Tagge CA, ZhangXL, Velisek L, Sullivan JA, Upreti C, Kracht JM, Ericsson M, Wojnarowicz MW, Goletani CJ, Maglakelidze GM, casey M, Moncaster JA, Minaeva O, Moir MD, Nowinski CJ, Stern RA, Cantu RC, Geiling J, Blustajn JK, Wolozin BL, Ikezu T, Stein TD, Budson AE, Kowall NW, Chargin D, Sharon A, Samans S, Hall GF, Moss WC, Cleveland RO, Tanzi RE, Stanton PK, McKee AC. Chronic traumatic encephalopathy in blast-exposed military veterans and a blast neurotrauma mouse model. Science Translational Medicine 2012; 4: 134ra60.doi:10.1126/scitranslmed.3003716

6 McKee AC, Stein TD, Nowinski CJ, Stern RA, Daneshvar DH, Alvarez VE, Lee HS, Hall G, Wojtowicz SM, Baugh CM, Riley DO, Kubilus CA, Cormier KA, Jacobs MA, Martin BR, Abraham CR, Ikezu T, Reichard RR, Wolozin BL, Budson AE,

Goldstein LE, Kowall NW, Cantu RC. The spectrum of disease in chronic traumatic encephalopathy. Brain 2013; 136: 43-64.doi:10.1093/brain/aws307

7 McKee AC, Daneshvar DH, Alvarez VE, Stein TD. The neuropathology of sport. Acta Neuropathol 2014; 127: 29-51.doi:10.1007/s00401-013-1230-6

8 Shetty AK, Mishra V, Kodali M, Hattiangady B. Blood brain barrier dysfunction and delayed neurological deficits in mild traumatic brain injury induced by blast shock waves. Front Cell Neurosci 2014; 8: No 232.doi:10.3389/fncel2014.00232

9 Hazrati LN, Taraglia MC, Diamandis P, Davis KD, Green RE, Wennberg R, Wong JC, Ezerins L, Tator CH. Absence of chronic traumatic encephalopathy in retired football players with multiple concussions and neurological symptomology. Front Hum Neurosci 2013; 7: No 222.doi:10.3389/fnhum.20B.00222

10 Randolph C. Is chronic traumatic encephalopathy a real disease? Curr Sports Med Rep 2014; 13: 33-37.doi:10.1249/JSR.0000000000000022

11 Saing T, Dick M, Nelson PT, Kim RC, Cribbs DH, Head E. Frontal cortex neuropathology in dementia pugilistica. J Neurotrauma 2012; 29: 1054-1070.doi:10.1089/neu.2011.1957

12 Stern RA, Daneshvar DH, Baugh CM, Selchepine DR, Montinegro PH, Riley DO, Fritts NG, Stamm JM, Robbins CA, McHale L, Simkin I, Stein TD, Alvarez VE, Goldstein LE, Budson AE, Kowall NW, Nowinski CJ, Cantu RC, McKee AC. Clinical presentation of chronic traumatic encephalopathy. Neurology 2013; 13: 1122-1129.

13 Montenigro PH, Baugh CM, Daneshvar DH, Mez J, Budson AE, Au R, Katz DI, Cantu RC, Stern RA. Clinical subtypes of chronic traumatic encephalopathy: literature review and proposed diagnostic criteria for traumatic encephalopathy syndrome. Alz Res & Therapy 2014; 6: No 68.doi:10.1186/s13193-014-0068-z14

14 McKee AC, Stein TD, Kieman PT, Alvarez VE. The neuropathology of chronic traumatic encephalopathy. Brain Pathol 2015a; 25: 350-364.doi:10.1111/bpa.12248

15 Kieman PT, Montinegro PH, Solomon TM, McKee AC. Chronic traumatic encephalopathy: A neurodegenerative consequence of repetitive brain injury. Sem Neurol 2015; 35: 20-28.doi:10.1055/s-oo35-1545080

16 Schmidt M, Zhukareva V, Newell L, Lee V, Trojanoswki J. Tau isoform profile and phosphorylation state in dementia pugilistica recapitulate Alzheimer's disease. Acta Neuropathol 2001; 101: 518-524.

17 Graham DI, Gentleman SM, Lynch A, Roberts GW. Distribution of beta-amyloid protein in the brain following severe head-injury. Neuropath Appl Neuro1995; 21: 27-34.doi:10.1111/j.1365-2990.1995.tb01025.x

18 Johnson VE, Stewart W, Smith DH. Widespread tau and amyloid-beta pathology many years after a single traumatic injury in humans. Brain Pathol 2012; 22: 142-149.doi:10.1111/j.1750-3639.2011.00513.x

19 Stein TD, Alvarez VE, McKee AC. Chronic traumatic encephalopathy: a spectrum of neuropathological changes following repetitive brain trauma in athletes and military personnel. Alz Res & Therapy 2014; 6: No 4.doi:10.1186alzrt234

20 Stein TD, Montenigro PH, Alvarez VE, Xia W, Crary JF, Tripodis Y, Daneshvar DH, Mez J, Soloman T, Meng G, Kubilus CA, Cormier KA, Meng KA, Babcock K, Kiernan P, Murphy L, Nowiski CK, Martin B, Dixon D, Stern RA, Cantu RC, Kowall NW, McKee AC. Beta-amyloid deposition in chronic traumatic encephalopathy. Acta Neuropathol 2015; 130: 21-34.doi:10.1007/s00401-015-1435-y

21 Braak H, Braak E. Argyrophilic grain disease: Frequency of occurrence in different age categories and neuropathologic diagnostic criteria. J Neural Transm 1998; 105: 801-819. doi:10.1007/s007020050096

22 Tolnay M, Monsch AU, Staehelin HB, Probst A. Argyrophilic grain disease: a disorder distinct from Alzheimer's disease. Pathologe 1999; 20: 159-168.doi:10.1007/s002920050339

23 Zhukareva V, Newell K, Lee V, Trojanowski J. Tau isoform profile and phosphorylation state in dementia pugilistica recapitulate Alzheimer's disease. Acta Neuropathol 2001; 101: 518-524.

24 Zhukareva V, Shah K, Uryu K, Braak H, del Tredici K, Sundarraj S, Clark C, Trojanowski JQ, Lee VMY. Biochemical analysis of tau proteins in argyrophilic grain disease, Alzheimer's disease and Pick's disease: a comparative study. Am J Pathol 2002; 161: 1135-1141.doi:10.1016/S0002-9440(10)64390-8

25 Sabbagh MN, Sandhu SS, Farlow MR, Veddeis L, Shell HA, Caviness JN, Connor DJ, Sue L, Adler CH, Beach TG. Correlation of clinical features with argyrophilic grains at autopsy. Alz Dis Assoc Disord 2009; 23: 229-233.

26 Ding ZT, Wang Y, Jiang YP, Hashizume Y, Yoshida M, Mimuro M, Inagaki T, Iwase T. Characteristics of alpha-synucleinopathy in centenarians. Acta Neuropathol 2006; 111: 450-458.doi:10.1007/s00401-005-0015-y

27 Josephs KA, Whitwell JL, Parisi JE, Knopman DS, Boeve BF, Geda YE, Jack CR, Petersen RC, Dickson DW. Argyrophilic grains: a distinct disease or an additive pathology? Neurobiol Aging 2008; 29: 566-573.doi:10.1016/j.neurobiolaging.2006.10.032

28 Cairns NJ, Bigio EH, Mackenzie IR, Neumann M, Lee VM, Hatanpaa KJ, White CL 3rd, Schneider JA, Grinberg LT, Halliday G, Duyckaerts C, Lowe JS, Holm IE, Tolnay M, Okamoto K, Yokoo H, Murayama S, Woulfe J, Munoz DG, Dickson DW, Ince PG, Trojanowski JQ, Mann DMA. Consortium for Frontotemporal Lobar

Degeneration. Neuropathologic diagnostic and nosologic criteria for frontotemporal lobar degeneration: consensus of the Consortium for Frontotemporal Lobar Degeneration. Acta Neuropathologica 2007; 114: 5-22.doi:10.1007/s00401-007-0237-2

29 Armstrong RA, Ellis W, Hamilton RL, Mackenzie IRA, Hedreen J, Gearing M, Montine T, Vonsattel J-P, Head E, Lieberman AP, Cairns NJ. Neuropathological heterogeneity in frontotemporal lobar degeneration with TDP-43 proteinopathy: a quantitative study of 94 cases using principal components analysis. J Neural Transm 2010; 117: 227-239.doi:10.1007/s00702-009-0350-6

30 Hyman BT, Phelps CH, Beach TG, Bigio EH, Cairns NJ, Carrillo MC, Dickson DW, Duyckaerts C, Frosch MP, Masliah E, Mirra SS, Nelson PT, Schneider JA, Thal DR, Thies B, Trojanowski JQ, Vinters HV, Montine TJ. National Institute on Aging-Alzheimer's Association guidelines for the neuropathologic assessment of Alzheimer's disease. Alz & Dement 2012; 8: 1-13.doi:10.1016/j.jalz2011.10.007

31 McKee AC, Cairns NJ, Dickson DW, Folkerth RD, Keene CD, Litvan I, Perl D, Stein TD, Vonsattel JP, Stewart W, Tripodis Y, Crary JF, Bienick KF, Dams-O'Connor K, Alverez VF, Gordon WA, the TBI/CTE group. The first NINDS/NIBIB consensus meeting to define neuropathological criteria for the diagnosis of chronic traumatic encephalopathy. Acta Neuropathol 2015b; DOI 10.1007/s00401-015-1515-z

32 Dickson DW. Neuropathology of non-Alzheimer degenerative disorders. Int J Clin Exp Pathol 2009; 3: 1-23

33 Crary JF, Trojanowski JQ, Schneider JA, Abisambra JF, Abner El, Alafuzoff I, Arnold SE, Attems J, Beach TG, Bigio EH, Cairns NJ, Dickson DW, Gearing M, grinberg LT, Hof PR, Hyman BT, Jellinger K, Jicha GA, Kovacs GG, Knopman PS, Kofler J, Kukull WA, McKenzie IR, Masliah E, McKee A, Montine TJ, Murray ME, Neltner JH, Santa Maria I, Seeley WW, Serramo-Pozo A, Shelanski ML, Stein T, Takao M, Thal DR, Toledo JB, Troncoso J, Vonsattel JP, White CL, wisniewski T,

Woltzer RL, Yamada M, Nelson PT. Primary age-related tauopathy (PART): a common pathology associated with human aging. Acta Neuropathol 2014; 128: 755-766.doi:10.0007/s00401-014-1349-0

34 Hof PR, Bouras C, Buee L, Delacourte A, Perl DP, Morrison JH. Differential distribution of neurofibrillary tangles in the cerebral cortex of dementia pugilistica and Alzheimer's disease cases. Acta Neuropathol 1992; 85: 23-30.

35 Snedecor GW, Cochran WG. *Statistical Methods*. Iowa State University Press, Ames, Iowa USA, 1980

36 Armstrong RA, Kotzbauer PT, Perlmutter JS, Campbell MC, Hurth KM, Schmidt RE, Cairns NJ. A quantitative study of α-synuclein pathology in fifteen cases of dementia associated with Parkinson disease. J Neural Transm 2014; 121: 171-181.doi:10.1007/s00702-013-1084-2

37 Armstrong RA, Cairns NJ, Lantos PL. Quantification of pathological lesions in the frontal and temporal lobe in ten patients diagnosed with Pick's disease. Acta Neuropathol 1999; 19: 64-70.

38 Armstrong RA, Cairns NJ, Lantos PL. A quantitative study of the pathological lesions in the neocortex and hippocampus of 12 patients with corticobasal degeneration. Exp Neurol 2000; 163: 348-356. doi:10.1006/exnr.2000.7392

39 Armstrong RA, Cairns NJ. Comparative quantitative study of 'signature' pathological lesions in the hippocampus and adjacent gyri of twelve neurodegenerative disorders. J Neural Transm 2015; 122: 1355-1367. Doi:10.1007/s00702-015-1402-8

40 Gentleman SM, Williams B, Roystan MC, Jagoe R, Clinton J, Perry RH, Ince PG, Allsop D, Polak JM, Roberts GW. Quantification of β/A4 protein deposition in the

medial temporal lobe: A comparison of Alzheimer's disease and senile dementia of the Lewy body type. Neurosci Lett 1992; 142: 9-12.doi:10.1016/0304-3940(92)90608-A

41 Armstrong RA. Quantitative differences in β/A4 protein subtypes in the parahippocampal gyrus and frontal cortex in Alzheimer's disease. Dementia 1994; 5: 1-5. doi:10.1159/000106686

42 Goedert M, Clavaguera F, Tolnay M. The propagation of prion-like protein inclusions in neurodegenerative diseases. Trends Neurosci 2010; 33: 317-325.doi:10.1016/j.tins.2010.04.003

43 Steiner JA, Angot E, Brundin P. A deadly spread: cellular mechanisms of α-synuclein transfer. Cell Death and Differ 2011; 18: 1425-1433.doi:10.1038.2011.53

Table 1. Demographic features and neuropathology features including National Institute on Aging-Alzheimer's association guidelines 'ABC' scores of the cases studied. Chronic traumatic encephalopathy cases also include frequency of traumatic incidents (first figure frequency of reported concussions, second figure concussions resulting in loss of consciousness), and sporting career length

Case	Age*	Duration (yrs)	Trauma (yrs)	Career length	Neuropathology	A	B	C
CTE								
A	75	10	10/2	18	CTE, ADNC, HS, TDP-43	A3	B2	C1
B	70	4	10/1	11	CTE, ADNC, TDP-43	A0	B2	C0
C	60	6	1/1	26	CTE,HS, TDP-43	A0	B1	C0
D	65	10	-	19	CTE,ADNC, HS,TDP-43	A2	B2	C1
E	70	8	3/0	21	CTE,TDP-43, PART,AGD	A0	B1	C0
F	80	15	F	12	CTE,ADNC, HS,TDP-43	A2	B2	C0
G	80	40	-	18	CTE,ADNC, TDP-43	A3	B2	C1
H	70	11	50/1	17	CTE/PART	A0	B2	C0
I	70	9	10/1	19	CTE,ADNC, TDP-43	A2	B1	C1
J	60	8	25/1	21	CTE,ADNC, TDP-43	A3	B2	C0
K	70	26	F	20	CTE	A0	B2	C0
ADNC								
A	90	5	-	-	ADNC	A3	B2	C1
B	70	3	-	-	ADNC/TDP-43	A2	B2	C1

C	80	5	-	-	ADNC/AGD	A0	B1	C0
D	85	12	-	-	ADNC/VD	A3	B2	C1
E	90	9	-	-	ADNC/TDP-43	A2	B1	C1
F	70	14	-	-	ADNC	A1	B2	C1
G	70	8	-	-	ADNC	A3	B2	C1

Abbreviations: F = Frequent, ADNC = Alzheimer's disease neuropathologic change, HS = Hippocampal sclerosis, TDP-43 = Transactive response (TAR) DNA-binding protein of 43kDa, PART = Primary age-related tauopathy, AGD = Argyrophilic grain disease, VD = Vascular disease, * Age rounded to nearest 5-year age interval to protect subject identities

Table 2. Mean densities (SE in parentheses) of tau–immunoreactive pathology (NFT, DN, DL, NP, AT, GI), together with abnormally enlarged neurons (EN), surviving neurons, and vacuoles in gyral crests/upper side of gyri and depths of sulci of various cortical regions (SFG = Superior frontal cortex, TP = Temporal pole, STG = Superior temporal gyrus, EC = Entorhinal cortex) in eleven cases of chronic traumatic encephalopathy.

		Cortical region			
Variable	Location	SFG	TP	STG	EC
NFT	Gyrus	0.59 (0.20)	1.73 (0.28)	0.95 (0.30)	1.69 (0.23)
	Sulcus	2.64 (0.68)	1.69 (0.26)	0.96 (0.20)	1.93 (0.30)
NT	Gyrus	1.30 (0.56)	1.96 (0.59)	1.63 (0.72)	3.39 (1.36)
	Sulcus	8.27 (1.84)	3.01 (0.69)	2.56 (0.59)	6.20 (1.55)
DL	Gyrus	8.45 (2.24)	20.88 (5.51)	12.58 (3.92)	22.25 (6.44)
	Sulcus	27.43 (5.09)	28.47 (3.57)	21.53 (5.84)	50.00 (8.16)
NP	Gyrus	0	0.002 (0.001)	0.01 (0.01)	0.01 (0.01)
	Sulcus	0.01 (0.01)	0.02 (0.01)	0.05 (0.03)	0
AT	Gyrus	0.11 (0.04)	0.20 (0.06)	0.15 (0.04)	0.21 (0.05)
	Sulcus	0.28 (0.08)	0.24 (0.07)	0.18 (0.04)	0.21 (0.07)
GI	Gyrus	0.02 (0.01)	0.01 (0.01)	0.02 (0.01)	0.01 (0.01)
	Sulcus	0.01(0.01)	0.02 (0.01)	0.02 (0.01)	0.01 (0.01)
EN	Gyrus	0.21 (0.04)	0.27 (0.05)	0.14 (0.03)	0.41 (0.09)
	Sulcus	0.29 (0.07)	0.29 (0.05)	0.13 (0.03)	0.28 (0.06)
Neurons	Gyrus	10.35 (1.00)	10.33 (1.12)	11.70 (0.81)	8.93 (1.15)
	Sulcus	10.43 (1.16)	11.66 (0.70)	12.05 (0.79)	10.96 (1.61)
Vacuoles	Gyrus	5.24 (0.68)	6.88 (1.58)	6.40 (1.06)	4.94 (1.55)
	Sulcus	4.19 (1.86)	4.61 (1.18)	4.27 (0.64)	3.94 (0.77)

Analysis of variance (ANOVA) (two-factor split-plot): NFT Region $F = 1.89$ ($P > 0.05$, Gyrus/Sulcus $F = 8.44$ ($P < 0.01$), Interaction $F = 6.64$ ($P < 0.001$); NT Region $F = 2.28$ ($P > 0.05$, Gyrus/Sulcus $F = 31.03$ ($P < 0.001$), Interaction $F = 7.11$ ($P < 0.001$); DL Region $F = 3.30$ ($P < 0.05$, Gyrus/Sulcus $F = 45.62$ ($P < 0.001$),

Interaction F = 4.06 ($P > 0.05$); AT Region F = 0.22 ($P > 0.05$, Gyrus/Sulcus F = 4.61 ($P < 0.05$), Interaction F = 1.69 ($P > 0.05$); GI Region F = 0.45 ($P > 0.05$, Gyrus/Sulcus F = 1.02 ($P > 0.05$), Interaction F = 0.51 ($P > 0.05$); EN Region F = 3.85 ($P < 0.05$), Gyrus/Sulcus F = 0.10 ($P > 0.05$), Interaction F = 2.19 ($P > 0.05$); Neurons Region F = 3.85 ($P < 0.05$), Gyrus/Sulcus F = 3.61 ($P > 0.05$), Interaction F = 0.81 ($P > 0.05$); Vacuoles Region F = 0.37 ($P > 0.05$, Gyrus/Sulcus F = 10.59 ($P < 0.01$), Interaction F = 0.52 ($P > 0.05$).

Table 3. Comparison of the densities of histological features (NFT = Neurofibrillary tangles, NT = Neuropil threads, DL = dot-like lesions, AI = Astrocytic inclusions, GI = Oligodendroglial inclusions, EN = abnormally enlarged neurons, N = Surviving neurons, V = vacuoles, NP = Neuritic plaques) in chronic traumatic encephalopathy (CTE) cases with those in Alzheimer's disease neuropathologic change (ADNC) not associated with CTE. Data are 'F' ratios from two-factor repeated-measures ANOVA (*P < 0.05, **P < 0.01, ***P < 0.001, ns = not significant, SFG = Superior frontal gyrus, AM = Amygdala)

Feature	Case group	Brain region	Interaction	*Post-hoc*
NFT	0.74 ns	5.32***	1.58 ns	ns
NT	1.82 ns	7.41***	2.02**	AD > CTE in STG,AM CTE > AD in CA2,CA4
DL	0.78 ns	10.05***	2.49**	CTE>AD in CA2,CA4, SFG
AT	5.26*	2.82***	1.07 ns	CTE > ADNC
GI	0.89 ns	0.92 ns	1.08 ns	ns
EN	0.04 ns	12.86***	1.44 ns	ns
N	3.26 ns	23.65***	1.41 ns	ns
V	1.54 ns	4.57*	0.70 ns	ns
NP	13.28**	3.83***	3.82***	AD > CTE especially in cortex

Table 4. Correlations (Pearson's 'r') between histological features (NFT = Neurofibrillary tangles, NT = Neuropil threads, DL = Grains, AT = Astrocytic inclusions GI = Oligodendroglial inclusions, EN = Abnormally enlarged neurons, N = Surviving neurons, V = Vacuolation) and the first two principal components (PC) in various brain regions (SFG = Superior frontal cortex, TP = Temporal pole, STG = Superior temporal gyrus, EC = Entorhinal cortex, G = Gyrus, CA1/2 = Sectors CA1-4 of the hippocampus, DG = Dentate gyrus, SN = Substantia nigra) in cases of chronic traumatic encephalopathy (* P < 0.05, ** P < 0.01). Only variables with at least one significant correlation with a PC are included

		PCA-1: All variables		PCA-2: Tau pathology	
Variable	Lesion	PC1	PC2	PC1	PC2
SFG (G)	V	-0.47	-0.34	-0.66*	-0.34
TP (G)	EN	0.58	0.27	0.64*	0.27
EC (G)	NFT	0.35	0.16	0.61*	0.16
EC (G)	GI	0.31	0.58	0.43	0.62*
CA1	NFT	0.01	0.63*	0.23	0.61*
CA1	DL	0.04	0.74**	0.24	0.73*
CA2	NT	-0.79**	-0.23	-0.68*	-0.25
CA4	NT	-0.63*	0.25	-0.48	0.23
DG	N	-0.28	0.66*	0.31	0.64*
DG	V	-0.62*	0.05	-0.31	0.06
SN	NT	-0.63*	0.33	-0.59	0.30
Career length		-0.26	-0.75**	-0.67*	-0.75**

Legends to figures

Fig 1. Tau-immunoreactive pathology in chronic traumatic encephalopathy (Arrow = Neurofibrillary tangle (NFT), Star = Neuropil thread (NT), Arrow head = Dot-like lesion (DL), tau immunohistochemistry (AT8), haematoxylin

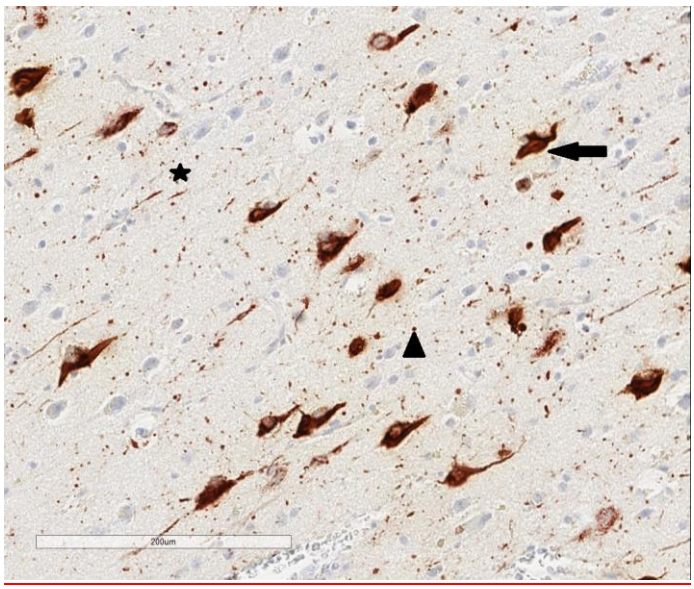

Fig 2. Cluster of astrocytic tangles (AT) (Arrow head) surrounding a blood vessel in the sulcus of the entorhinal cortex in chronic traumatic encephalopathy, tau immunohistochemistry (AT8), haematoxylin

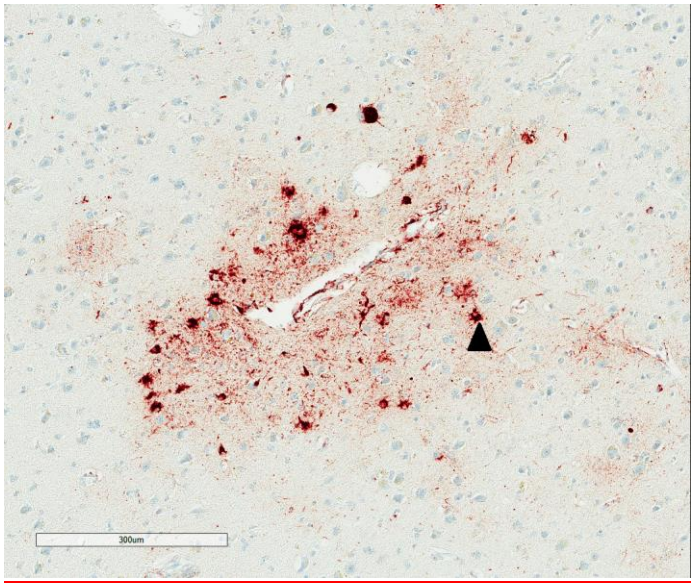

Fig 3. Abnormally enlarged neurons (EN) (Arrow head) and oligodendroglial inclusion (GI) (Arrow) in the superior frontal cortex in chronic traumatic encephalopathy, tau immunohistochemistry (AT8), haematoxylin

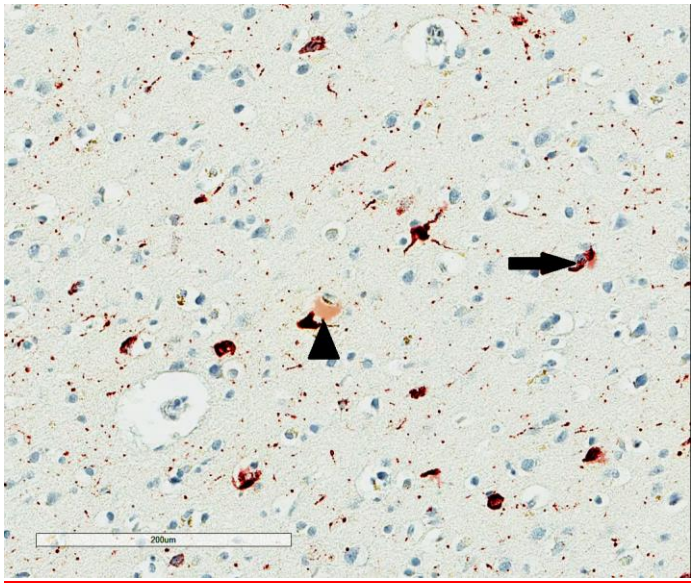

Fig 4. Vacuolation of the neuropil (Arrows), in the superior frontal cortex in chronic traumatic encephalopathy, tau immunohistochemistry (AT8), haematoxylin

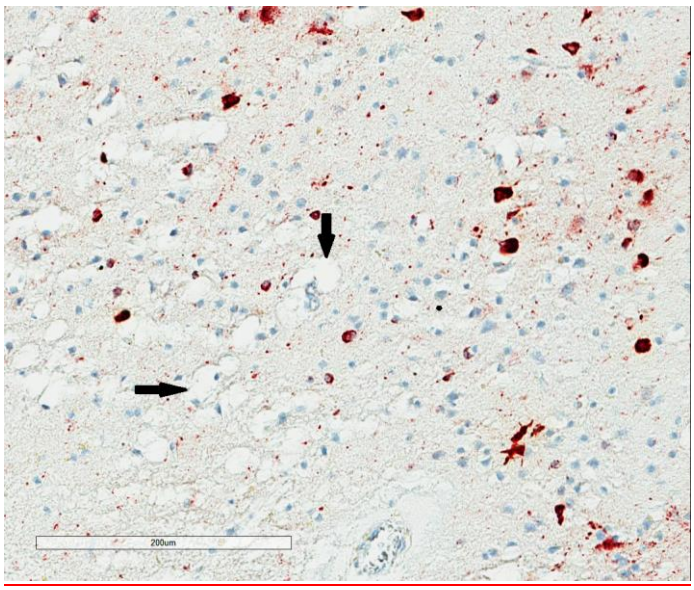

Fig 5. Densities of tau–immunoreactive neuronal pathology (NFT, NT, DL, NP) in various brain regions (SFG = Superior frontal cortex, TP = Temporal pole, STG = Superior temporal gyrus, EC = Entorhinal cortex, Sub = Subiculum, CA1-4 = Cornu ammonis sectors of the hippocampus, DG = Dentate gyrus, AM = Basolateral amygdala, SN = Substantia nigra) in cases of chronic traumatic encephalopathy. Analysis of variance (ANOVA): Two-way, (NFT $F = 4.42$ ($P < 0.01$); NT $F = 3.49$ ($P < 0.001$), DL $F = 4.56$ ($P < 0.001$); NP $F = 0.40$ ($P > 0.05$)

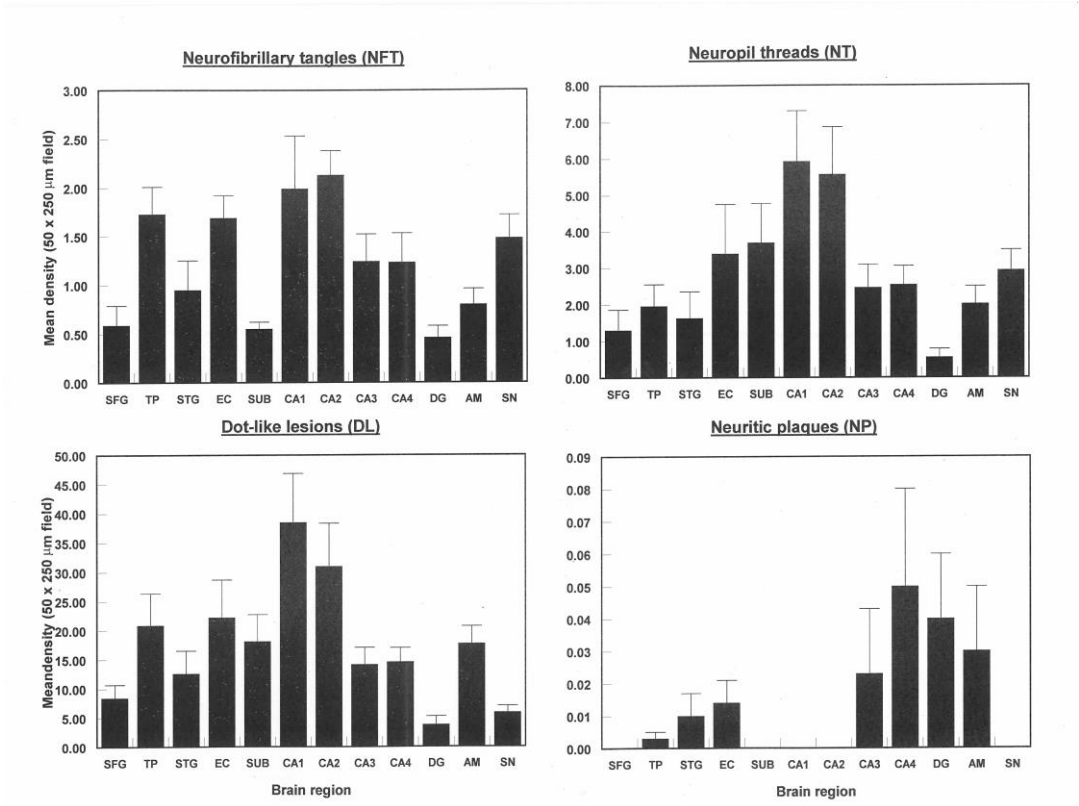

Fig 6. Densities of tau–immunoreactive glial pathology (AT, GI) in various brain regions (SFG = Superior frontal cortex, TP = Temporal pole, STG = Superior temporal gyrus, EC = Entorhinal cortex, Sub = Subiculum, CA1-4 = Cornu ammonis sectors of the hippocampus, DG = Dentate gyrus, AM = Basolateral amygdala, SN = Substantia nigra) in cases of chronic traumatic encephalopathy. Analysis of variance (ANOVA): Two-way, (AT F = 1.58 (P > 0.05); GI F = 1.10 (P > 0.05)

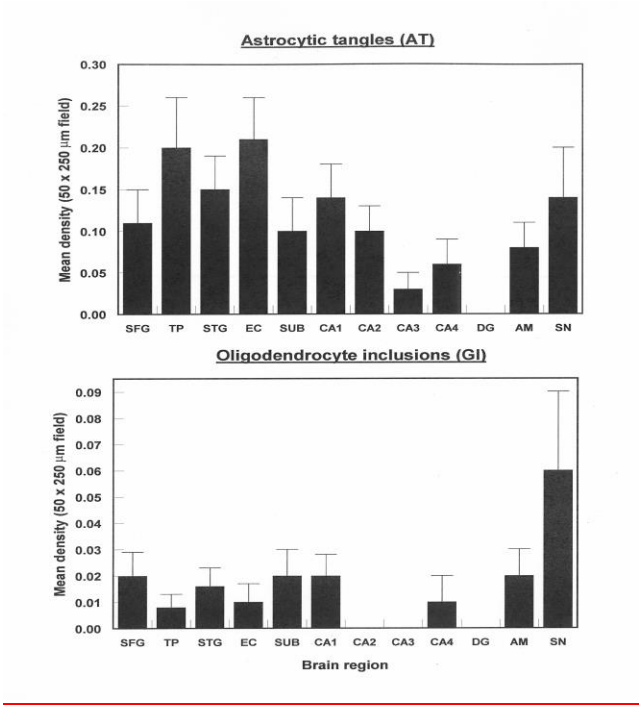

Fig 7. Densities of abnormally enlarged neurons (EN), and vacuoles (V) in various brain regions (SFG = Superior frontal cortex, TP = Temporal pole, STG = Superior temporal gyrus, EC = Entorhinal cortex, Sub = Subiculum, CA1-4 = Cornu ammonis sectors of the hippocampus, DG = Dentate gyrus, AM = Basolateral amygdala, SN = Substantia nigra) in cases of chronic traumatic encephalopathy. Analysis of variance (ANOVA): Two-way, (EN $F = 6.81$ ($P < 0.001$); V $F = 3.81$ ($P < 0.001$).

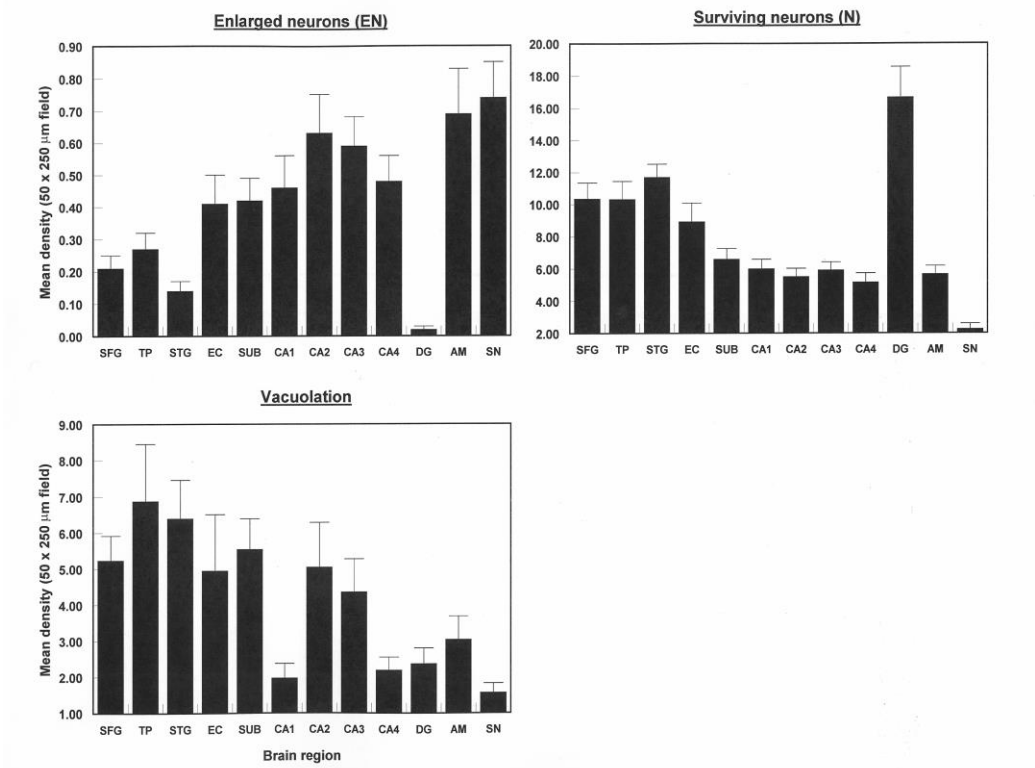

Fig 8. Principal components analysis (PCA) of eleven cases of chronic traumatic encephalopathy based on all histological variables (PCA-1). A plot of cases in relation to PC1 and PC2. The various co-morbidities are plotted in relation to each case (AD = Alzheimer's disease neuropathological change, AGD = Argyrophilic grain disease, PART = Primary age-related tauopathy, HS = Hippocampal sclerosis, TDP = transactive response (TAR) DNA-binding protein of 43kDa (TDP-43)-immunoreactive pathology)

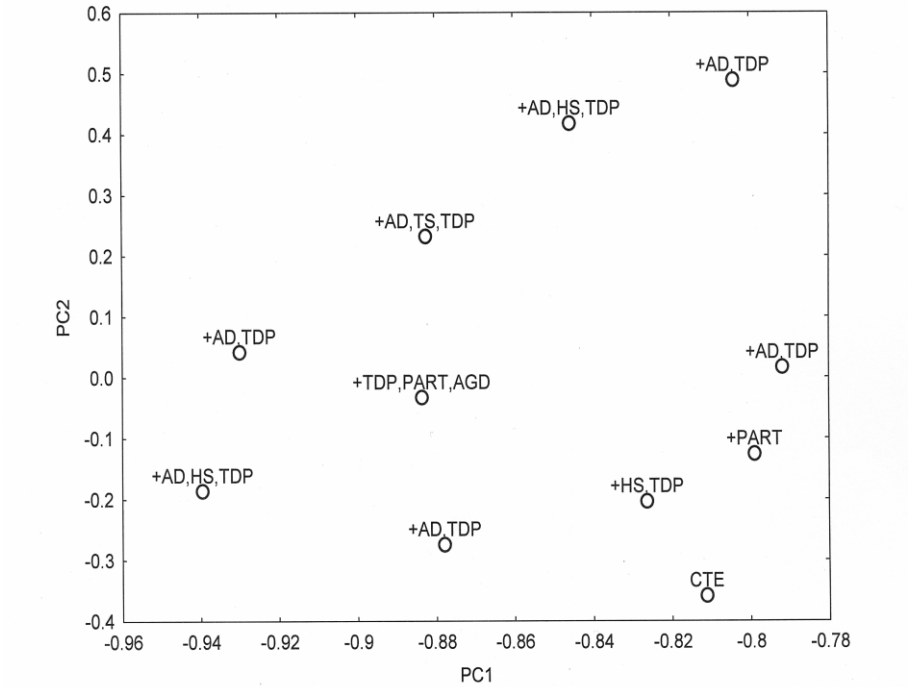

Fig 9. Principal components analysis (PCA) of eleven cases of chronic traumatic encephalopathy based on tau-immunoreactive pathology only (NFT, NT, DL, AI, GR, NP) (PCA-2). A plot of cases in relation to PC1 and PC2. Duration of sporting career in years is plotted in relation to each case.